engineering proceedings

MDPI

Proceedings Paper

Estimation of Building Heights and DEM Accuracy Assessment Using ICESat-2 Data Products †

G Pavan Sai Goud [1,*] and Dr. Ashutosh Bhardwaj [2]

[1] Department of Urban and Regional Studies, Indian Institute of Remote Sensing, Indian Space Research Organization, Dehradun, Uttarakhand, India
[2] Photogrammetry, and Remote Sensing Department, Indian Institute of Remote Sensing, Indian Space Research Organization, Dehradun, Uttarakhand, India; ashutosh@iirs.gov.in
* Correspondence: goddupavansaigoud@gmail.com
† Presented at 8th International Electronic Conference on Sensors and Applications, 1–15 November 2021; Available online: https://ecsa-8.sciforum.net.

Abstract: Urban monitoring using remote sensing is the most reliable and cost-effective method that provides high accuracy and multi-temporal data for studying urban expansion in horizontal and vertical dimensions. Vertical monitoring of urban areas includes mapping compactness, population growth, and study of urban surface geometry, which plays an essential role in the applications of urban heat islands, generation of urban canopy layer, etc. The presented study uses the Ice, cloud, and land elevation satellite-2 (ICESat-2) ATL 03 photon data for building height estimation for a sample of 30 buildings in three experimental sites. The heights computed from the ICESat-2 laser altimeter-based profile were compared with google images of respective buildings for the accuracy assessment. The results when compared to the ICESat-2 reference data give an RMSE of 2.04 m. Another popular way to map the vertical dimension of terrain in urban areas that are globally used by policymakers for resource management, planning, and maintenance is the Digital Elevation Model (DEM). It can be generated using various remote sensing techniques but the usage of active remote sensing procedures has an advantage over passive methods due to their capability to function both day and night irrespective of weather. Thus, the study further aims to assess the openly accessible DEM products available from TanDEM-X, which is a German Earth observation satellite that uses InSAR (Synthetic Aperture Radar Interferometry) technique, and Cartosat-1, an optical stereo acquisition satellite launched by the Indian Space Research Organization (ISRO), which uses satellite photogrammetry. Taking ICESat-2 (ATL-08) Elevation data as reference, the accuracy of two study sites was checked by statistical measures such as Mean error (ME), Mean absolute error (MAE), Root mean square error (RMSE). In the urban area of Greater Hyderabad Municipal Corporation (GHMC), an RMSE of 5.29m and 7.48m were observed for TanDEM-X 90 and CartoDEM V3 R1 respectively, while the TanDEM-X 90 and CartoDEM V3 R1 showed an RMSE of 5.15 and 5.48 in the Bellampalli Mandal rural site respectively. The DEMs exhibited better results for the Bellampalli Mandal rural area of Telangana State as the built-up is sparse and the terrain is mostly flat as compared to the GHMC site. The results show that the accuracy of TanDEM-X is better as compared to the CartoDEM V3 R1. These results can assist the decision-makers and planners in choosing suitable DEMs for planning and management purposes for smart cities as well as rural settlements.

Keywords: ICESat-2; laser altimetry;TanDEM-X; Cartosat-1; InSAR; urban monitoring

Citation: Goud, P; Bhardwaj, A. Estimation of Building Heights and DEM Accuracy Assessment Using ICESat-2 Data Products. *Eng. Proc.* **2021**, *3*, x. https://doi.org/10.3390/xxxxx

Academic Editor:

Published: 1 November 2021

1. Introduction

Digital Elevation Model (DEM) is used globally by policymakers for resource management, planning, and maintenance. It can be processed to extract information about the earth's topography and has applications in various fields. DEM can be generated using various remote sensing techniques, using active remote sensing DEMs like TanDEM-X

and SRTM missions, and by using optical stereo missions like Cartosat-1, ASTER, and ALOS PRISM which were launched for DEM generation as one of the aims and are openly accessible. Availability of openly accessible DEMs has increased and thus there is a need for analyzing the quality of DEMs with quantitative accuracy assessment techniques for better results. The TanDEM-X mission with its alike satellite TerraSAR-X (TSX) radar satellite is flying in a close orbit and has a major objective to generate high-precision DEM in the bistatic mode. The Cartsosat-1 satellite is equipped with two high-resolution cameras (PAN-Fore or the frontward-looking camera and PAN-Aft or the afterword-looking camera) capable of providing imagery of 2.5m spatial resolution. Validation of these openly available DEMs is going on and various researchers had done accuracy assessments over different terrains, comparing different types of DEMs values against the highly precise ground points globally (e.g., GPS, NASA ICESat/GLAS) [1–5] or reference DEMs[6,7]. ICESat-2/GLAS data were selected often due to its distribution of signal photons from pole to the pole which has high accuracy and widespread coverage [5,8,9]. However, the accuracy of ICESat-2 is influenced by ground slope for larger areas, so it is not always suitable to validate the accuracy of DEMs [5].

A DEM captures latitude, longitude, and elevation information of the earth's surface and can be viewed either as a raster or in the form of a vector dataset known as Triangulated Irregular Network (TIN) [7] and it can be represented in a gridded model [10,11]. DEMs are now readily and openly available which makes easy access to the data for use in various applications. Ever since the availabilities of various models, it is necessary to examine the quality of them through quantitative methods for better use in different applications and areas [10]. The DEM can be processed through Geographical Information System (GIS) software to extract information about the earth's topography including contours, slope, and elevation, hydrology including surface water flow and watershed, and geomorphology. DEM products have applications in various fields such as cartography and mapping [1,4,12], terrain analysis, urban planning, agriculture and forestry [13,14], vulnerability analysis [15,16], watershed planning, and drainage modeling [17–19], atmospheric aerosol estimation [20], soil conditions modeling [17,21], archaeological exploration [22] and defense [23]. DEMs can be generated using a variety of sources and methods such as digitization of contours, Radio-echo sounding surveys, Airborne ice-penetrating radar techniques, Three-dimensional seismic survey, Satellite radar altimetry, Airborne optical sensing, Laser surveys, and Conventional topographic surveys [24].

Urban monitoring using Remote sensing (RS) is the most reliable and cost-effective method, which provides high accuracy and multitemporal data for urban mapping (infrastructure mapping, Slums identification, mapping of vulnerable areas prone to disasters, etc) and urban monitoring at different scales. Urban monitoring generally includes both horizontal and vertical change [25]. Vertical monitoring of urban areas to derive the compactness, population growth, and one major indicator to study the urban surface geometry, and acts an essential role in the fields like urban heat islands, generation of urban canopy layer, etc [8,25–27]. Horizontal monitoring can be achieved using low, medium, and high-resolution satellites images, whereas vertical monitoring requires high-resolution satellite data where several new techniques have been used such as optical stereophotogrammetry, InSAR, and airborne LiDAR, ICESat-2/GLAS, etc. [8,25,28–31].

The present study was to estimate the building heights using ICESat-2 ATL 03 data. It further examines the quality of Cartosat-1 and Tandem-X DEMs over Urban and Rural areas. For building height estimation over 3 different sites, 30 samples were collected and compared with google images which were considered for reference height. Two locations one urban and one rural were selected for assessment of the accuracy of these DEMs using highly accurate ICESat-2 altimetry data. The Urban area selected consists of highly dense built-up and the Rural area selected for experimentation has mostly flat terrain with sparse built-up.

2. Materials and Methods

2.1. Digital Elevation Model

A Digital Elevation Model (DEM) is a mathematical representation of the terrain or the topographic surface [32–34]. The study uses the CartoDEM version 3 release 1 (V3 R1) data from National Remote Sensing Centre (NRSC) and TanDEM-X 90 dataset from the German Space Agency (DLR).

2.2. CARTOSAT-1 Mission

The Cartosat-1 was launched by the Indian Space Research Organization (ISRO), the eleventh of the IRS series, at the Satish Dhawan Space Centre (SDSC) in Sriharikota. The satellite is positioned in the polar Sun Synchronous Orbit at an altitude of 618 km from the Earth [35]. The satellite became the first global stereo-capable satellite to be launched with a spatial resolution of 2.5m and was unique in its ability to provide high-resolution panchromatic stereoscopic images [36]. The Cartsosat-1 satellite is equipped with two high-resolution cameras (PAN-Fore or the frontward-looking camera and PAN-Aft or the afterward-looking camera) capable of providing imagery of 2.5 m spatial resolution with a b/h ratio of 0.62. The cameras are positioned with mount angles of +26° and −5° respectively and are engineered using modern technologies to collect along-the-track stereo imagery with swaths of 30 km (Fore) and 27 km (Aft) and a base-to-height ratio of 0.62 [3]. The major specifications of this satellite mission and the planned products are tabulated in Table 1.

Table 1. Cartosat-1 Satellite Mission specifications.

S. No.	Parameter	Specification
1	Nominal Altitude	618 km
2	Spatial Resolution	2.5 m
3	Radiometric Resolution	10 bits
4	Swath	30 km (Fore), 27 km (Aft)
5	Product Dimensions	30 km × 30 km
6	Local time for equatorial crossing	10:30 AM
7	Instantaneous Geometric Field of View (IGFOV)	2.5 × 2.7 m (Fore) 2.22 × 2.23 m (Aft)
8	Spectral Bands No. of bands Bandwidths	 1 Panchromatic 0.5–0.85 μ
9	Quantization	10 bits/pixel
10	No. of detectors	12,000/camera
11	Base-Height Ratio	0.62
12	Planimetric Accuracy	15 m (CEP90)
13	Vertical Accuracy	8 m (LE90)
14	National Level DEM	CartoDEM
15	Processing Tools	SAPHIRE 1.0

Major utilization of the Cartosat-1 imagery is in the production of Digital Elevation Models (DEMs) of the earth's terrain and Cartography.

2.3. TanDEM-X DEM

The TanDEM-X mission with its alike satellite TerraSAR-X (TSX) radar satellite (in space since June 2007) is flying in close orbit with a baseline of 250–500 m formation with adjustable scenarios in both cross and along-track directions, it is to achieve the desired interferometric baselines and the major objective is to generate a DEM at a global level

which is steady, timely, and with high-precision in the bistatic mode [37–39]. Thus bistatic interferometry transmits pulses from one of the satellite's antennae and receives the backscattered signals at the same time from two satellites, which reduces the impacts of substantial temporal decorrelation and atmospheric disturbances of the old repeat-pass InSAR on the procurement of highly accurate cross-track interferograms [5]. This project completed the imaging of the earth at least twice, with extra scope over the areas of complex topography, and it also took into account of relocation of the orbits for avoiding radar shadowing in difficult terrains [40]. Freely accessible TanDEM-X 90 DEM (90 m) is used for the present study and the specifications are given in Table 2.

Table 2. Specifications of TanDEM-X 90 products.

S. No.	Specifications of TanDEM-X	TanDEM-X
1	Acquisition technique	RADAR
2	Data format	GeoTIFF
3	Vertical datum	WGS84 ellipsoidal heights
4	Spatial resolution	90 m
5	Projection system	Geographic
6	Absolute horizontal accuracy (CE90)	below 10 m
7	Absolute Vertical accuracy	below 10 m
8	Relative vertical accuracy for slopes at or below 20%	2 m
9	Relative vertical accuracy for slopes above 20%	4 m

2.4. ICESat-2

The Ice, Cloud, and land Elevation Satellite (ICESat-1) was in operation from 2003 to 2009, the first-ever spaceborne laser altimetry mission for Earth science. This mission uses laser altimetry for determining elevation changes of glaciers, ice sheets, and sea ice thickness distribution [41]. From recommendations by the National Research Council for an ICESat consequent mission, the ICESat-2 mission was launched on 15 September 2018 [5]. ICESat-2 has a multi-beam instrument design known as the Advanced topographic laser altimeter system (ATLAS) which hosts a photon-counting technology. ATLAS Splits into 6 beams set as 3 pairs of beams, all these beam pair consists of a strong and weak energy beam (4:1 ratio), the major specifications shown in Table 3 below.

Though the ATLAS instrument is enhanced as a global mission to measure changes in polar ice and land ice thickness, ICESat-2 collects elevation data for all surfaces, from pole to pole by the distribution of signal photons, the ATL08 algorithm gives Land Water Vegetation Elevation which consists of elevation heights along with canopy surface. It also includes canopy cover percentage, surface slope, surface roughness, canopy height, and apparent reflectance [8,9]. As it is providing quality and sufficient reference data, it is suitable for accurate analysis of different DEMs. Neuenschwander et al. in their research carried out a quantitative evaluation of the terrain heights of the ICESat-2 ATL-08 products comparing with airborne lidar data where the results have shown a Mean absolute error (MAE) of 0.5 m, while Root Mean Square Error (RMSE) was 0.82 m. The study proved that it is reasonably suitable for use as reference data for the accuracy assessment of DEMs [5,42,43].

ICESat-2 ATL 03 acquires the data containing a global geolocated photon representing the surface elevation detected by the ATLAS sensor, accurate latitude, longitude, with elevation data for each photon, organized by the beam in the along-track direction. These photons were classified by signal versus background including the type of surface with all geophysical corrections, segmented into numerous minute granules [9]. The evaluation of vertical accuracy reported by the various researchers through efficient evaluation is in

the range of 2 to 50 cm which is acceptable for urban studies for building height estimation [8].

Table 3. ICESat-2 Specifications.

S. No.	Mission	ICESat-2
1	Launch date	15 September 2018
2	Nominal Duration	3 years
3	Detector	Hamamatsu photomultiplier
4	Detector type	Photon counting
5	Wavelength	532 nm (green)
6	Orbit inclination and Coverage	92°; coverage up to 88°N–88°S latitude
7	Track number	6 tracks from 1 laser
8	Acquisition strategy	3 pairs (a strong and a weak beam) created by beam-splitting optics in the laser transmitter
9	Laser power	120 μJ/30 μJ
10	Footprint diameter	~12 m
11	along-track spacing	~0.7 m
12	across-track spacing	90 m within pairs, 3.3 km between pairs

2.5. Study Area

Samples for building height estimation were collected from three different sites namely Hyderabad, Paris, and Vancouver. The rationale for selecting these sites for assessment is the availability of many suitable ICESat-2 ground tracks over three sites and the availability of google images for those respective buildings which were attached in Appendix-A. A total of 30 buildings that were distributed over the three study areas have been collected shown in Table 4. The sample buildings were selected based on the availability of geolocated photons that fall on the bare Earth, which is treated as the local datum and which also has significant geolocated photons falling on the building's roof.

Table 4. Details of the buildings with their position on the beams of ICESat-2 ground track.

Place	Building. No.	Track Id/Beam Id/Date of Acquisition	Building Position on the Beam (Lat., Long.)
Hyderabad	1	t1148/gt3l/2020-12-08	17.4390056, 78.4751239
	2	t653/gt2r/2020-02-07	17.4631615, 78.3737838
	3	t653/gt1r/2021-02-04	17.4430168, 78.3768220
	4	t1148/gt2r/2019-06-12	17.4371660, 78.4828767
	5	t1148/gt1l/2020-12-08	17.4234564, 78.3408120
	6	t1148/gt3r/2020-03-10	17.4349488, 78.5320913
	7	t1148/gt2r/2019-06-12	17.4748731, 78.3930326
	8	t653/gt2r/2020-02-07	17.4364234, 78.3760944
	9	t653/gt2r/2020-02-07	17.4393428, 78.3754439
	10	t653/gt2r/2020-02-07	17.4504948, 78.3732881
	11	t1148/gt2r/2021-03-09	17.4351007, 78.3859719
	12	t653/gt3r/2018-11-10	17.4162568, 78.3705803
	13	t653/gt2r/2018-11-10	17.3997395, 78.3425604
Paris	14	t938/gt3l/2019-02-27	48.8293113, 2.2523981
	15	t938/gt3l/2019-02-27	48.8881962, 2.2604336
	16	t938/gt3l/2019-02-27	48.8588103, 2.2980711
	17	t938/gt3r/2019-02-27	48.9020286, 2.2614291

	18	t938/gt3l/2019-02-27	48.9105713, 2.2638678
	19	t778/gt2l/2019-02-17	48.8873445, 2.1694545
	20	t938/gt1l/2019-02-27	48.8774477, 2.3467241
	21	t938/gt1l/2019-02-27	48.9032770, 2.3509193
	22	t778/gt2r/2019-02-17	48.8777919, 2.1716283
Vancouver	23	t1050/gt1l/2020-12-01	49.3155437, −122.9708216
	24	t1050/gt2r/2021-04-19	49.1890883, −123.0790622
	25	t1050/gt3r/2020-12-01	42.2848871, −123.0660846
	26	t1050/gt3l/2020-09-02	49.2750352, −123.1312038
	27	t387/gt1r/2021-04-19	49.3198650, −123.0952621
	28	t387/gt3r/2021-04-19	49.2617017, −122.7767959
	29	t1050/gt1l/2019-09-04	49.2817339, −123.1380390
	30	t1050/gt1l/2019-09-04	49.2912939, −123.1367726

For comparison of DEMs (TanDEM-X 90 and CartoDEM V3 R1) over urban and rural areas, two study areas have been chosen one is Greater Hyderabad Municipal Corporation (Urban area) and another Bellampalli Mandal (Rural area) of Telangana state as shown in Figure 1.

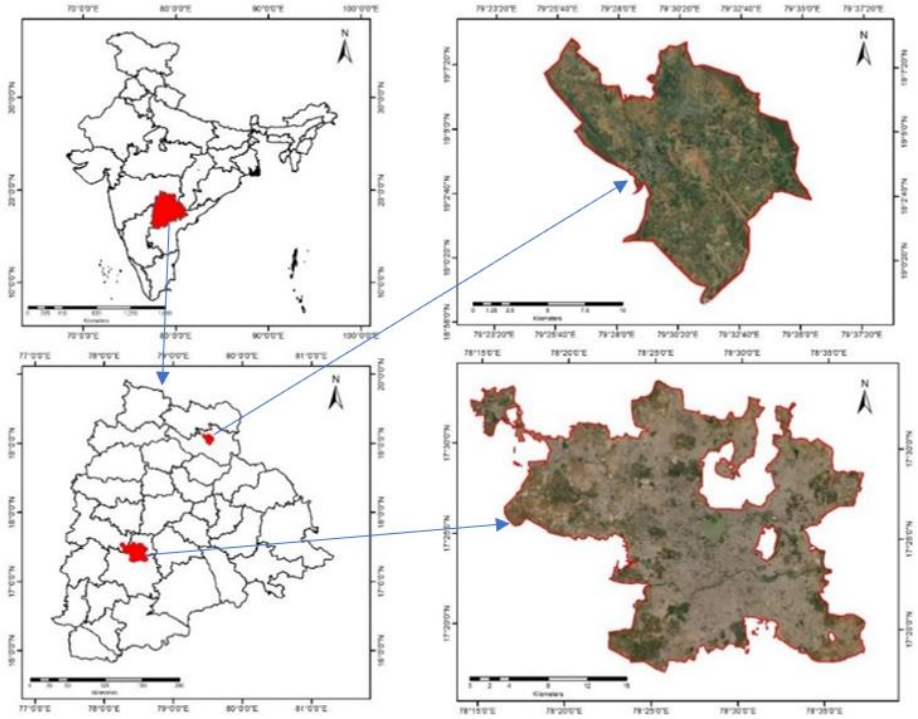

Figure 1. Map showing study area locations of GHMC and Bellampalle Mandal.

2.5.1. Greater Hyderabad Municipal Corporation (GHMC)

The study area lies at around 17.3850° N, 78.4867° E, and is the capital city of Telangana State, spread over an area of 650 km^2. It is one of the largest municipal corporations with a population of 7.9 million. The city is situated in the Deccan Plateau and has an average height of 536 m above mean sea level. It is the IT hub of Telangana where it attracts lots of migrants from other states for employment purposes leading to the rapid growth of the city, resulting in a densely built, and populous metropolitan area.

2.5.2. Bellampalli Mandal

Bellampalli is a Mandal in Mancherial District of Telangana State lies at 19.0715° N, 79.4912° E, noted for its coal mines Singareni Collieries Company Limited, spread over an area of 35.06 km². It is a fertile plain with the Godavari River flowing through the district and the majority of the population in the area is agriculture-dependent.

2.6. Methodology

Online visualization and downloading facility for various ICESat-2 data products in a.csv format are provided in the web portal called openAltimetry, with an option for 3D visualizing of the data [8,9]. For this study ICESat-2, ATL 03 data has been downloaded for three site areas. ATL03 data product provides the data of geolocated photons with their heights along with the time of acquisition. ATL03 classifies each photon based on their confidence levels which range from 0–4 and are represented as noise, buffer, low, high, medium, on which one can understand either an unaffected signal photon event or a noise photon event; where 4 indicating an event with a high level of confidence and 0 implying noise. The data product ATL03 undertakes several geophysical corrections which are related to atmosphere, tidal and solid Earth deformation and provides corrected heights for all the photon events [8]. The methodology followed in this study is shown in Figure 2.

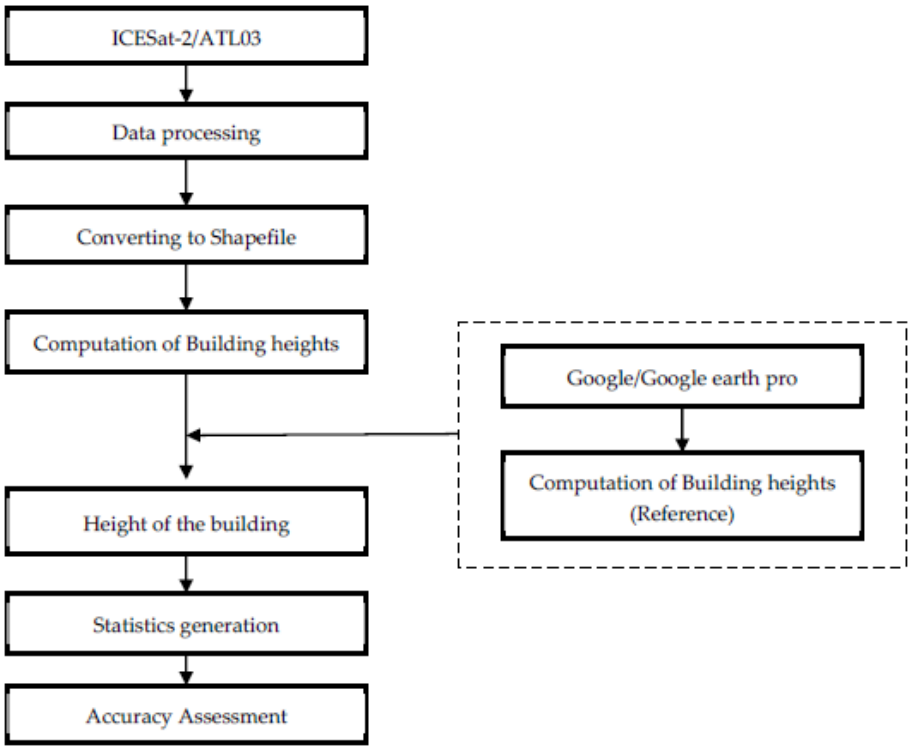

Figure 2. Flowchart for building height estimated using ICESat-2 ATL03.

$$Height\ of\ the\ building\ =\ Elev_{bldg}\ -\ Elev_{ref} \quad (1)$$

For the assessment of DEMs, TanDEM-X 90 and CartoDEM datasets were downloaded from the respective websites for both study areas GHMC (Urban) and Bellampalli (Rural) shown in Figures 7 and 8. ATL 08 product of ICESat-2 has been collected in .csv format from NSIDC shown in Table 5, which was utilized for evaluation of the TanDEM-X 90 DEM and CartoDEM V3 R1 over the two experimental sites of Urban and Rural areas. A study on ALT 08 data has revealed that it provides terrain elevation with vertical accu-

racy ranges between 1 cm to 49 cm [8]. However, outliers causing poor acquisition conditions such as clouds are filtered before using the product. The methodology followed is shown in Figure 3.

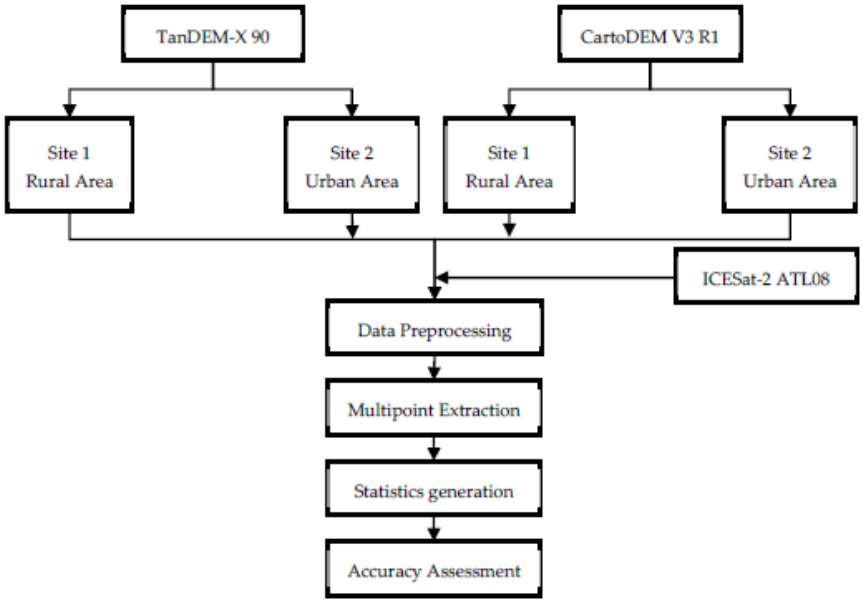

Figure 3. Flowchart for Accuracy Assessment of Openly accessible DEMs.

The statistical parameters such as Mean Absolute Error (MAE), Standard Deviation (SD), Mean Error (ME), and Root Mean Square Error (RMSE) were calculated for quality assessment of DEMs. MAE is mathematically linear where the RMSE is quadratic and has a relatively high weight to large errors because the errors are squared before averaging [6,10]. The difference between the value of the respective height from the TanDEM-X 90 m and CartoDEM V3 R1 ($Zi_{(DEM)}$) products; and the reference height from ICESat-2 ATL08 ($Zi_{(REF)}$) was computed. Accordingly, RMSE is used to measure the vertical accuracy. The ME (Equation 2), MAE (Equation 3), and RMSE (Equation 4) were calculated using respective equations.

$$ME = \frac{\sum_{i=0}^{n} Zi_{(DEM)} - Zi_{(REF)}}{n} \quad (2)$$

$$MAE = \frac{\sum_{i=0}^{n} \left| Zi_{(DEM)} - Zi_{(REF)} \right|}{n} \quad (3)$$

$$RMSE = \sqrt{\frac{\sum_{i=1}^{n} (Zi_{(DEM)} - Zi_{(REF)})^2}{n}} \quad (4)$$

here, n equals to no. of observations available for validation

Table 5. Description of selected ICESat 2 data.

Location	Product	Trcak_ID	Year	No. of Data Sets	Format
GHMC	ATL 08, ATL 03	1148	2018–2021	7	.CSV
Bellampalle	ATL 08	1089 and 142	2018–2021	16	.CSV

Figure 4. Distribution of ICESat-2 tracks: (**a**) GHMC Site; (**b**) Bellampalle Site overlaid on google earth images.

3. Results and Discussion

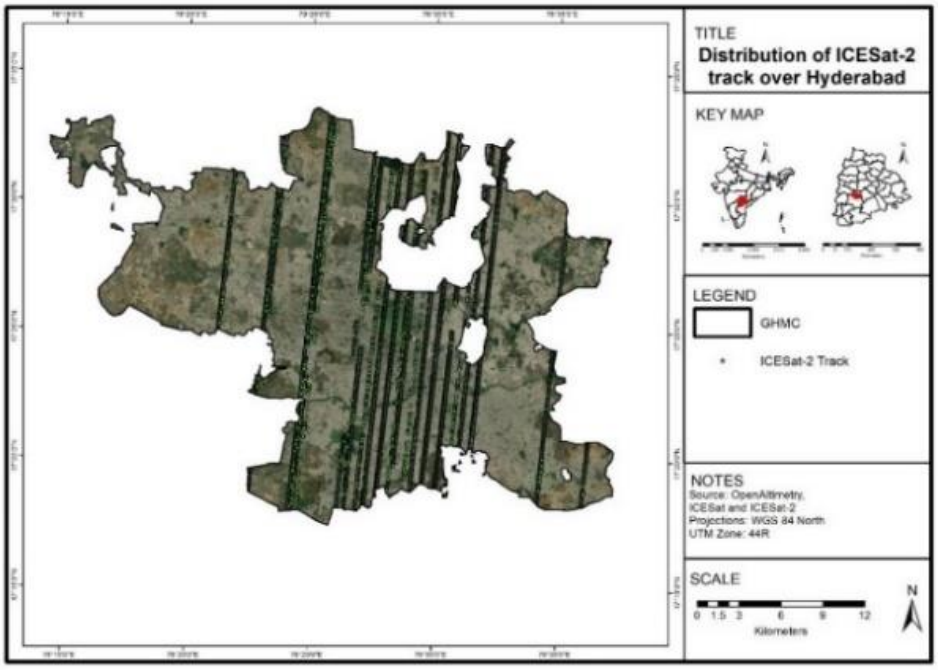

(**a**)

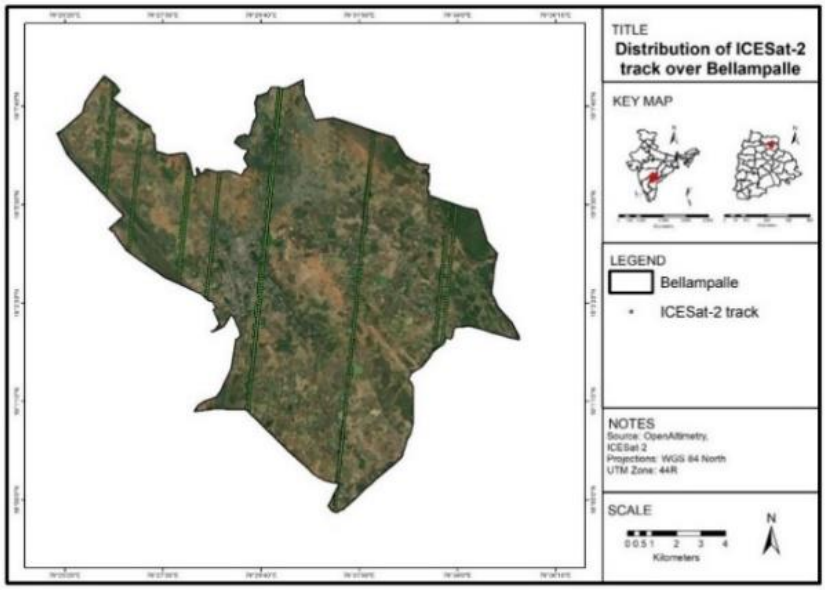

(**b**)

Mean elevation from the building surface ($\boldsymbol{Elev_{bldg}}$) and mean elevation from the adjoining bare ground (datum) ($\boldsymbol{Elev_{ref}}$) were computed and the height estimation is done using Equation (1). No. of floors for each building were identified and multiplied with an assumed average floor height of 3 m, which is considered as reference height of buildings as shown in Figures 5 and 6. RMSE and percentage error were calculated for evaluation of ICESat-2 data which are shown in Table 6. RMSE is not always a good indicator for describing average model performance in specific situations and gives more

weight to larger errors [6,10], so percentage error is carried out for individual samples since the height of the sampled buildings varying from 6m to 150 m.

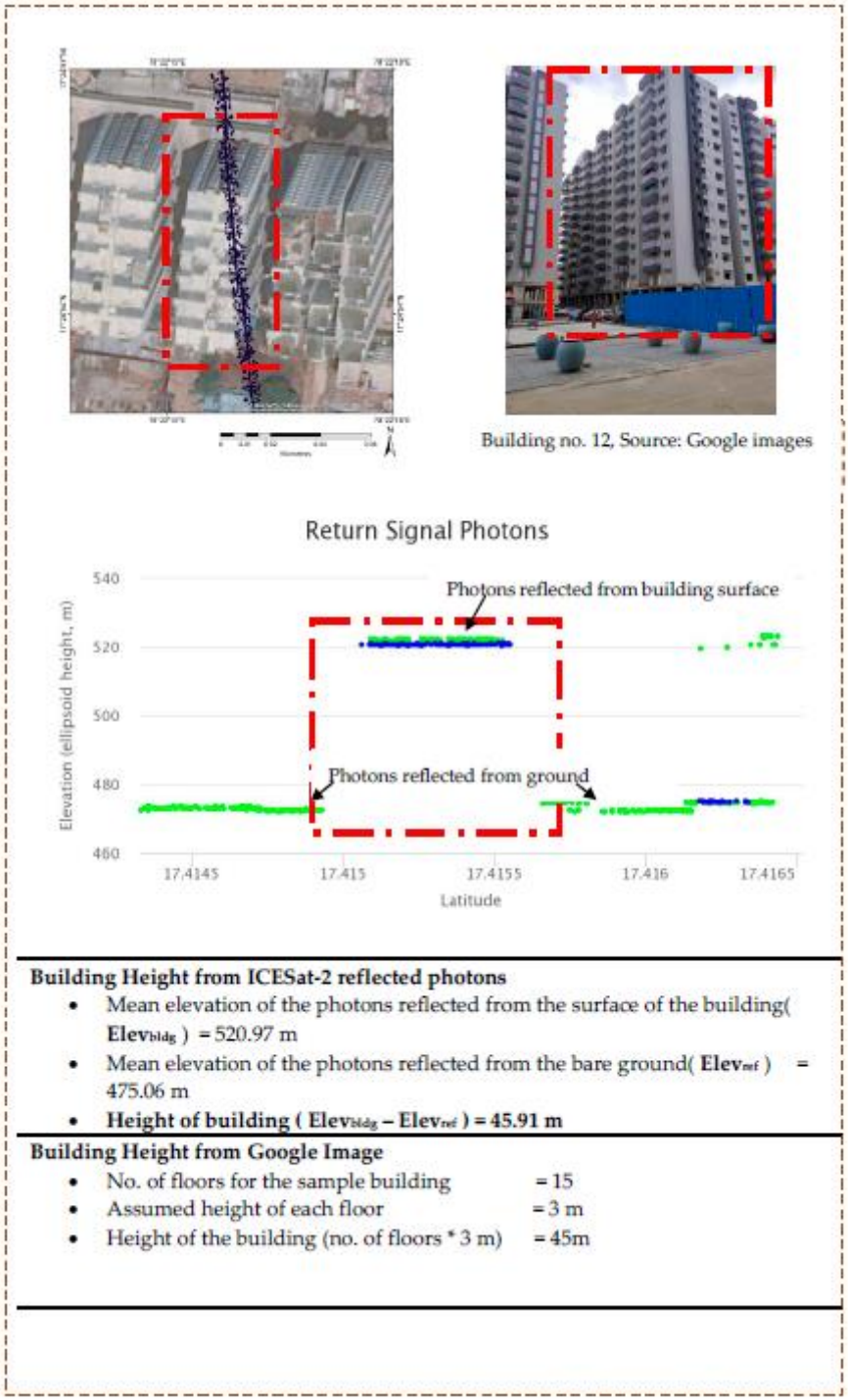

Figure 5. Measurement of one sample building for height estimation.

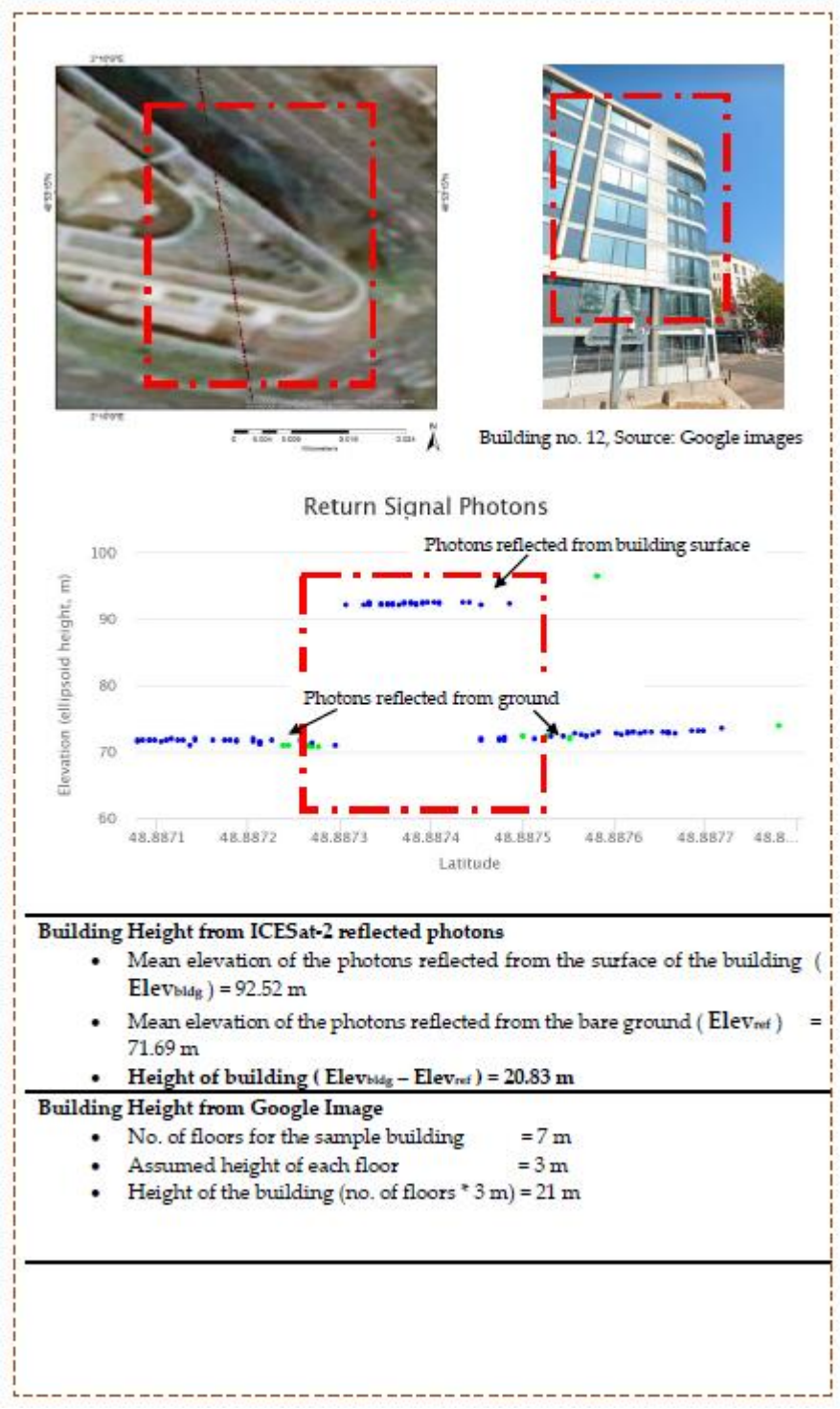

Figure 6. Measurement of sample building for height estimation.

Table 6 shows the mean elevation calculated from the reflected photons from the building's roof surface and adjacent bare ground as shown in columns 2 and 3. The height computed from ICESat-2 profile, google photographs are shown in columns 4 and 5, whereas the height difference calculated using equation 1 between these two estimates is shown in column 6 with the percentage error of each sample building in column 7. The difference values for the building height estimation are ranging from 0.01 m to 3.7 m, and the percentage error varying from 0.004% to 28%. It is observed that either overestimation or underestimation of buildings heights exist in computations. Since the heights of the

buildings are calculated from the mean elevation of the building's surface and the adjoining mean elevation of the bare ground (datum), the uncertainties from these two can affect the building height estimation. The architectural aspect of the building is also not considered when the assumed floor height is multiplied by the no. of floors identified. The photons of both medium and high confidence levels were considered which also affected the estimation to an extent.

Table 6. Statistical details of the sample buildings resulting from the ICESat-2 profiles and reference heights along with the height difference and percentage error.

Building. No.	Mean Elevation of the Building (Elevbldg.) m	Mean Elevation of the Adjacent Bare Earth (Elevref) m	Heights of the Building Computed from ICESat-2 Profile	Heights of the Building Computed Using Google Photos	Height Difference	% Error
1	468.01	444.96	23.05	21.00	2.05	10%
2	566.38	510.81	55.57	54.00	1.57	3%
3	565.54	521.89	43.66	42.00	1.66	4%
4	495.70	450.48	45.22	45.00	0.22	0%
5	545.55	480.02	65.53	66.00	−0.47	1%
6	455.05	445.92	9.13	10.00	−0.87	9%
7	600.75	500.86	99.89	100.00	−0.11	0%
8	593.15	492.81	100.34	105.00	−4.66	4%
9	532.02	512.13	19.89	18.00	1.89	11%
10	552.79	531.12	21.67	18.00	3.67	20%
11	558.97	507.86	51.11	48.00	3.11	6%
12	520.97	475.06	45.91	45.00	0.91	2%
13	504.15	464.87	39.29	39.00	0.29	1%
14	101.46	74.92	26.55	24.00	2.55	11%
15	96.45	72.90	23.55	21.00	2.55	12%
16	107.60	87.06	20.54	21.00	−0.46	2%
17	115.05	83.06	31.99	30.00	1.99	7%
18	109.81	85.30	24.51	24.00	0.51	2%
19	92.52	71.69	20.83	21.00	−0.17	1%
20	106.94	82.23	24.71	21.00	3.71	18%
21	102.58	84.18	18.40	18.00	0.40	2%
22	86.13	73.90	12.23	15.00	−2.77	18%
23	114.48	81.48	33.00	33.00	−0.0019	1.5%
24	−1.93	−17.87	15.94	18.00	−2.06	11%
25	−2.15	−13.37	11.22	9.00	2.22	25%
26	147.61	−5.35	152.96	150.30	2.66	2%
27	−3.56	−11.21	7.65	6.00	1.65	28%
28	−9.25	−15.30	6.05	6.00	0.05	1%
29	58.45	−1.07	59.52	60.00	−0.48	1%
30	30.24	−0.01	30.25	33.00	−2.75	8%

Figure 7. TanDEM-X: (**a**) GHMC Site; (**b**) Bellampalle Site.

Table 7 describes the statistical evaluation of TanDEM-X 90 and CartoDEM V3 R1 with the ICESat-2 ATL 08 elevation data for the study sites of GHMC and Bellampalle

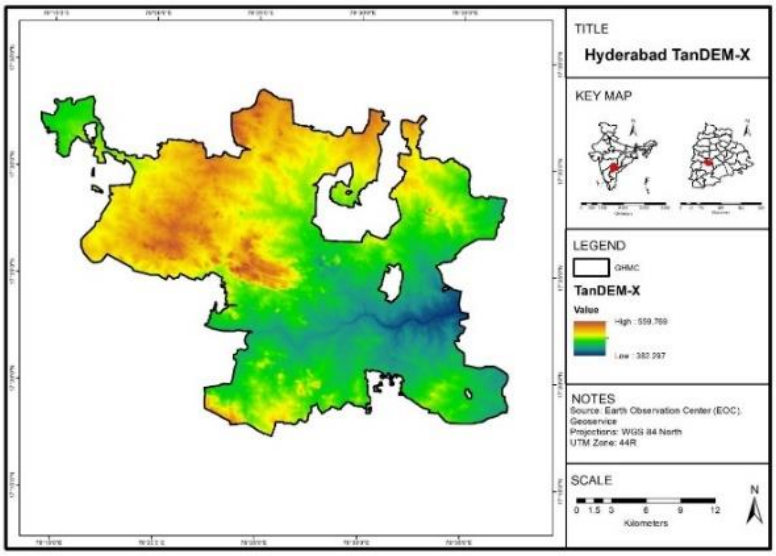

(**a**)

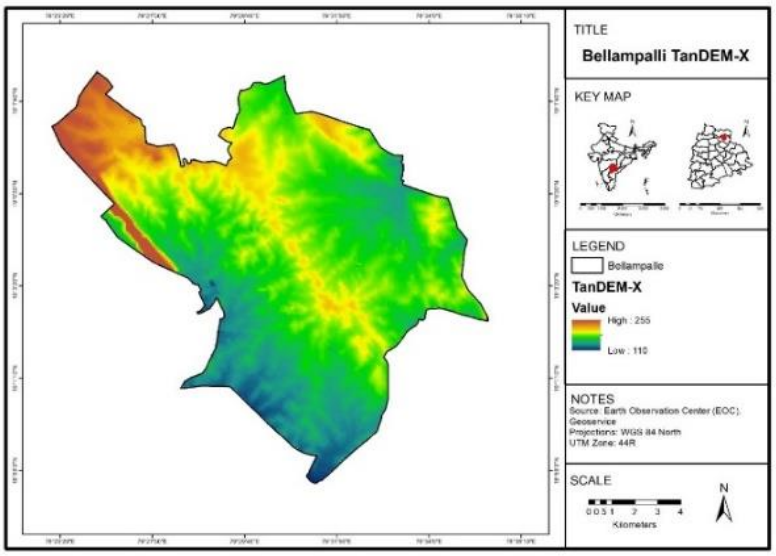

(**b**)

Mandal. ME, MAE, and RMSE reveal that the TanDEM-X DEM performs better both in Urban and Rural areas with RMSE as 5.29 m and 3.12 m in comparison to CartoDEM V3 R1 having RMSE of 7.48 m and 3.32 over Urban and Rural areas respectively. However, GHMC, the urban area selected for the study consists of high dense built-up that tends to result in a higher RMSE for the CartoDEM due to the considerations of photogrammetry. On the other hand, both the DEMs exhibited better results for the Bellampalli Mandal rural area of Telangana State as the built-up is sparse and the terrain is mostly flat. As observed in various studies RMSE is not always a good indicator for describing average model performance in specific situations and influences by larger errors, and thus the MAE can measure better statistics for average error [6,10].

Figure 8. Cartosat-1 DEM: (**a**) GHMC Site; (**b**) Bellampalle Site.

Table 7. Statistical parameters for DEMs for the Urban and Rural areas.

MAE for the study areas GHMC, and Bellampalli are 3.7 m and 1.4 m for TanDEM-X 90 DEMs, whereas its 6.2 m, and 2.1 m for CartoDEMs for Urban and Rural areas respectively depicting higher accuracies in rural areas. LE90 can be calculated directly from

Site	DEMs	ME	MAE	RMSE	LE90	SD	Skew
GHMC (Urban)	TanDEM-X	3	3.7	5.29	8.73	4.38	0.23
	CartoDEM	6	6.2	7.48	12.34	4.49	1.25
Bellampalle (Rural)	TanDEM-X	0.9	1.4	3.12	5.14	2.99	5.4
	CartoDEM	1.8	2.1	3.32	5.48	2.77	8.25

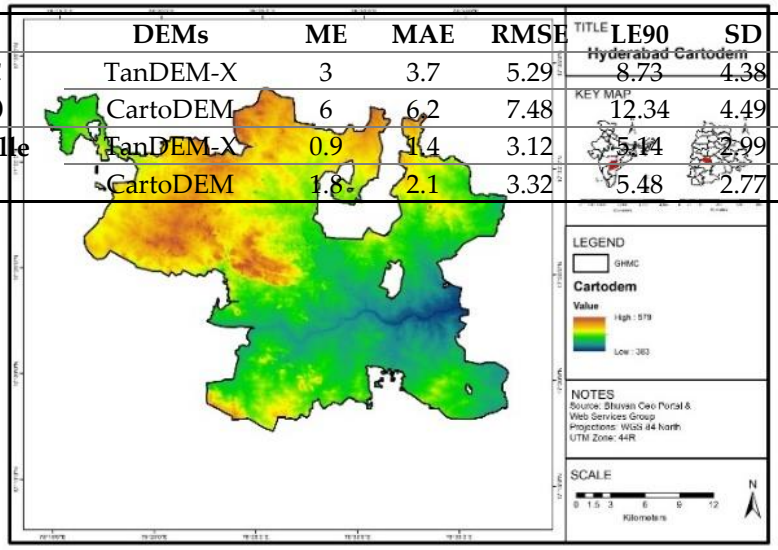

(**a**)

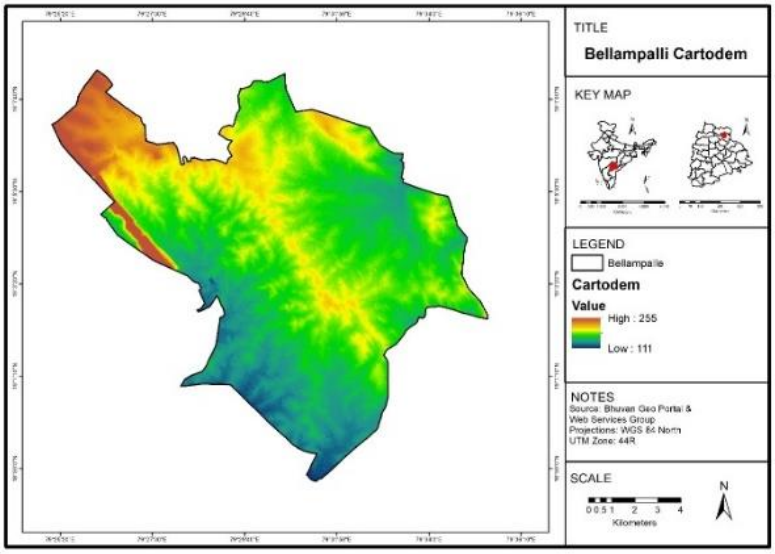

(**b**)

RMSE (LE90 = 1.65 × RMSE)[6] for both the test sites. The RMSE was found greater than 5 m as observed for the two DEMs. TanDEM-X for urban area site is relatively symmetric, where CartoDEM V3 R1 showed positively skewed distribution as per the calculated coefficient of Skewness (Skew) in Table 7.

The results varied based on the uncertainties such as the confidence level of photon events, computations from the mean value from building surfaces and bare ground, and the reference heights of the building. The presence of water tanks, solar panels, network towers, or any such materials on the buildings can affect the photon signals, and show the higher elevation when compared to the actual height of the building. The accuracy estimations can further be higher when the reference building heights are collected from the ground surveys and by using the photon events of confidence level 4. The openly accessible DEMs are having variability in the quality over different regions (Urban and Rural) in this study and also over different terrains so it is required to understand the purpose of the study or application to decide which DEMs are required and can give better accuracy for the models [10,38].

4. Conclusions

The study showcases the building height estimations successfully in urban and rural areas using ICESat-2 ground tracks and its ATL 03 data. The statistical results are reasonably acceptable for buildings with a higher number of floors, considering all the uncertainties for reference building height. 70% of the sampled buildings have a percentage error below 10%, with 30% of the buildings having above 10% especially for buildings ranging from 2 to 5 floors. ICESat-2 data due to its along-track and discrete nature cannot be a general solution for height estimation of all buildings. The DEMs were evaluated with ICESat-2 ATL 08 Elevation data, concluding that TanDEM-X DEMs having higher accuracies in both the Urban and Rural regions under study. Both the DEMs exhibited better results for the Bellampalli Mandal rural area of Telangana State as the built-up is sparse and the terrain is mostly flat. This result can assist the decision-makers and planners in choosing suitable DEMs for planning and management purposes and the utilization of ICESat-2 ATL 03 data for higher confidence levels and technological advantages.

5. Acknowledgment

The authors would like to thank ISRO, NASA, ESA, and Google LLC for their support to the researchers through openly accessible data-sharing platforms. The authors are highly indebted to Director, IIRS for his constant support and encouragement in conducting the research activities.

Institutional Review Board Statement:

Informed Consent Statement:

Data Availability Statement:

Appendix A


Building 1
Building 2
Building 3
Building 4
Building 5
Building 6
Building 8
Building 9
Building 7
Building 10
Building 16
Building 11
Building 12
Building 13
Building 15
Building 20
Building 14
Building 17
Building 18
Building 23
Building 25
Building 19
Building 29
Building 30
Building 22
Building 21
Building 26

References

1. Gianinetto, M.; Milano, P.; Leonardo, P.; Vinci, D. Multi-Scale Digital Terrain Model Generation Using Cartosat-1 Stereo Images for the Mausanne Les Alpilles Test Site. *Archives* **2006**, *3*, 1331–1336.
2. Winograd, M. Environmental indicators for Latin America and the Caribbean: Toward land-use sustainability. *IICA-GTZ Proj. Inter-Am. Inst. Coop. Agric.* **1995**, *83*.
3. Srivastava, P.K. Recent Advances in Cartosat-1 Data Processing. ISPRS Hann. Work. 2007. Available online: https://www.isprs.org/proceedings/XXXVI/1-W51/paper/Srivastava_etal.pdf (accessed on).
4. Rao, C.V.; Sathyanarayana, P.; Jain, D.S.; Manjunath, a.S. Topographic Map Updation Using Cartosat-1 data. 2007. Available online: (accessed on).
5. Liu, Z.; Zhu, J.; Fu, H.; Zhou, C.; Zuo, T. Evaluation of the vertical accuracy of open global dems over steep terrain regions using icesat data: A case study over hunan province, china. *Sensors* **2020**, *20*, 1–16, doi:10.3390/s20174865.
6. Bhardwaj, A. Quality Assessment of Openly Accessible Fused EarthEnvDEM90 DEM and its Comparison with MERIT DEM Using Ground Control Points for Diverse Topographic Regions. *MOL2NET Int. Conf. Ser. Multidiscip. Sci.*, 6th ed.; 2020; pp. 1–8. Available online: https://sciforum.net/paper/view/conference/6855 (accessed on).
7. Krishnan, S.; Sajikumar, N.; Sumam, K. DEM Generation Using Cartosat-I Stereo Data and its Comparison with Publically Available DEM. *Procedia Technol.* **2016**, *24*, 295–302, doi:10.1016/j.protcy.2016.05.039.
8. Dandabathula, G.; Sitiraju, S.R.; Jha, C.S. Retrieval of building heights from ICESat-2 photon data and evaluation with field measurements. *Environ. Res. Infrastruct. Sustain.* **2021**, *1*, 011003, doi:10.1088/2634-4505/abf820.
9. Data Products ICESat-2. Available online: https://icesat-2.gsfc.nasa.gov/science/data-products (accessed on 21 August 2021).
10. Bhardwaj, A. Assessment of Vertical Accuracy for TanDEM-X 90 m DEMs in Plain, Moderate, and Rugged Terrain. *Proceedings* **2019**, *24*, 8, doi:10.3390/iecg2019-06208.
11. Ventura, S.J.; Grams, S.A.; Wechsler, S.P. Perceptions of Digital Elevation Model Uncertainty by DEM Users. *Urban Reg. Inf. Syst. Assoc.* **2003**, *15*.
12. Gianinetto, M. Evaluation of Cartosat-1 multi-scale digital surface modelling over france. *Sensors* **2009**, *9*, 3269–3288, doi:10.3390/s90503269.
13. Kay, S.; Zielinski, R. Orthorectification and geometric quality assessment of Cartosat-1 for common agricultural policy monitoring. *Int. Arch. Photogramm. Remote Sens. Spat. Inf. Sci.* **2006**, *XXXVI*, 6.
14. Avtar, R.; Sawada, H. Use of DEM data to monitor height changes due to deforestation. *Arab. J. Geosci.* **2013**, *6*, 4859–4871, doi:10.1007/s12517-012-0768-2.
15. Kumar, T.S.; Mahendra, R.S.; Nayak, S.; Radhakrishnan, K.; Sahu, K.C. Coastal vulnerability assessment for Orissa State, East Coast of India. *J. Coast. Res.* **2010**, *26*, 523–534, doi:10.2112/09-1186.1.
16. Fereshtehpour, M.; Karamouz, M. DEM Resolution Effects on Coastal Flood Vulnerability Assessment: Deterministic and Probabilistic Approach. *Water Resour. Res.* **2018**, *54*, 4965–4982, doi:10.1029/2017WR022318.
17. Case, B.S.; Meng, F.-R.; Arp, P.A. Digital elevation modelling of soil type and drainage within small forested catchments. *Can. J. Soil Sci.* **2005**, *85*, 127–137, doi:10.4141/S04-008.
18. Bandyopadhyay, S.; Srivastava, S.K.; Jha, M.K.; Hegde, V.S.; Jayaraman, V. Harnessing earth observation (EO) capabilities in hydrogeology: An Indian perspective. *Hydrogeol. J.* **2007**, *15*, 155–158, doi:10.1007/s10040-006-0122-4.
19. Singh, P.; Gupta, A.; Singh, M. Hydrological inferences from watershed analysis for water resource management using remote sensing and GIS techniques. *Egypt. J. Remote Sens. Sp. Sci.* **2014**, *17*, 111–121, doi:10.1016/j.ejrs.2014.09.003.
20. Pandya, M.R. Estimation of aerosol optical thickness over land using dual angle panchromatic data. *Remote Sens. Atmos. Clouds* **2006**, *6408*, 64080X, doi:10.1117/12.693948.
21. Murphy, P.N.C.; Ogilvie, J.; Arp, P. Topographic modelling of soil moisture conditions: A comparison and verification of two models. *Eur. J. Soil Sci.* vol. 60, no. 1, pp. 94–109, 2009, doi:10.1111/j.1365-2389.2008.01094.x.
22. Rajani, M.B. The expanse of archaeological remains at Nalanda: A study using remote sensing and GIS. *Arch. Asian Art* **2016**, *66*, 1–23, doi:10.1353/aaa.2016.0010.
23. van Persie, M.; Noorbergen, H.H.S.; van den Broek, a.C.; Dekker, R.J. Use of Remote Sensing Imagery for Fast Generation of Military Maps and Simulator Databases. *Simulation* **2000**, *XXXIII*, 573–581.
24. Florinsky, I. Digital Terrain Analysis in Soil Science and Geology. *Digit. Terrain Anal. Soil Sci. Geol.* 2012, 31–41, doi:10.1016/C2010-0-65718-X.
25. Yang, X.; Wang, C.; Xi, X.; Wang, P.; Lei, Z.; Ma, W.; Nie, S. Extraction of Multiple Building Heights Using ICESat/GLAS Full-Waveform Data Assisted by Optical Imagery. *IEEE Geosci. Remote Sens. Lett.* **2019**, *16*, 1914–1918, doi:10.1109/LGRS.2019.2911967.
26. Why Satellites Are the Future of Urban Planning Earth-i. Available online: https://earthi.space/blog/future-urban-planning/ (accessed on 19 July 2021).
27. Bande, S.; Shete, V.V. Smart flood disaster prediction system using IoT & neural networks. *Proc. 2017 Int. Conf. Smart Technol. Smart Nation, SmartTechCon* **2018**, 189–194, doi:10.1109/SmartTechCon.2017.8358367.

28. Sonde, P.; Balamwar, S.; Ochawar, R.S. Urban sprawl detection and analysis using unsupervised classification of high resolution image data of Jawaharlal Nehru Port Trust area in India. *Remote Sens. Appl. Soc. Environ.* **2020**, *17*, 100282, doi:10.1016/j.rsase.2019.100282.
29. Hegazy, I.R.; Kaloop, M.R. Monitoring urban growth and land use change detection with GIS and remote sensing techniques in Daqahlia governorate Egypt. *Int. J. Sustain. Built Environ.* **2015**, *4*, 117–124, doi:10.1016/J.IJSBE.2015.02.005.
30. Jagadish, K. Urban Sprawl Pattern Recognition and Modeling Using GIS. 2014. Available online: https://www.researchgate.net/publication/237816205 (accessed on July 19 2021).
31. Jat, M.K.; Garg, P.; Khare, D. Monitoring and modelling of urban sprawl using remote sensing and GIS techniques. *Int. J. Appl. Earth Obs. Geoinf.* **2008**, *10*, 26–43.
32. Li, Z.; Zhu, Q.; Gold, C. *Digital Terrain Modeling : Principles and Methodology*; CRC Press: Boca Raton, FL, USA, 2005.
33. USGS, What is a digital elevation model (DEM)? 2021. Available online: https://www.usgs.gov/faqs/what-a-digital-elevation-model-dem?qt-news_science_products=0#qt-news_science_products (accessed on).
34. Bhardwaj, A.; Jain, K.; Chatterjee, R.S. Generation of high-quality digital elevation models by assimilation of remote sensing-based DEMs. *J. Appl. Remote Sens.* **2019**, *13*, 1, doi:10.1117/1.JRS.13.4.044502.
35. Murthy, Y.V.N.K.; Rao, S.S.; Rao, D.S.P.; Jayaraman, V. Analysis of DEM generated using Cartosat-1 stereo data over Mausanne Les Alpiles–Cartosat scientific appraisal programme (CSAP TS–5). *Int. Arch. Photogramm. Remote Sens. Spat. Inf. Sci.* **2008**, *37*, 1–6.
36. Muralikrishnan, S.; Narender, B.; Reddy, S.; Pillai, A. Evaluation of Indian National DEM from Cartosat-1 data. *Indian Sp. Res. Organ.* **2011**, *1*, 1–19. Available online: http://bhuvan-noeda.nrsc.gov.in/download/download/tools/document/CartoDEMReadme_v1_u1_23082011.pdf (accessed on).
37. TDX (TanDEM-X)-eoPortal Directory-Satellite Missions. eoPortal Directory. 2021. Available online: https://earth.esa.int/web/eoportal/satellite-missions/t/tandem-x#SG9SE1157Herb (accessed on).
38. Tridon, D.B.; Bachmann, M.; Boer, J.; Bräutigam, B.; Gonzalez, C.; Kraus, T.; Krieger, G.; Martone, M.; Polimeni, M.D.; Schulze, D.; et al. COMPARISON OF TANDEM-X AND CARTOSAT-1 STEREO DEMS OVER DIFFERENT TERRAINS OF INDIA Rinki Deo, Minal Jain and Y.S. Rao Centre of Studies in Resources Engineering , Indian Institute of Technology Bombay. *2016 IEEE Int. Geosci. Remote Sens. Symp.* **2016**, 6484–6487.
39. Tridon, D.B. TanDEM-X going for the DEM: Acquisition, performance, and further activities. In Proceedings of the 2015 IEEE 5th Asia-Pacific Conf. Synth. Aperture Radar, APSAR 2015, January 2017; pp. 163–168, doi:10.1109/APSAR.2015.7306180.
40. Grohmann, C.H. Evaluation of TanDEM-X DEMs on selected Brazilian sites: Comparison with SRTM, ASTER GDEM and ALOS AW3D30. *Remote Sens. Environ.* **2018**, *212*, 121–133, doi:10.1016/j.rse.2018.04.043.
41. Markus, T.; Neumann, T.; Martino, A.; Abdalati, W.; Brunt, K.; Csatho, B.; Farrell, S.; Fricker, H.A.; Gardner, A.; Harding, D.; et al. The Ice, Cloud, and land Elevation Satellite-2 (ICESat-2): Science requirements, concept, and implementation. *Remote Sens. Environ.* **2017**, *190*, 260–273, doi:10.1016/j.rse.2016.12.029.
42. Neuenschwander, A.L.; Magruder, L.A. The ATL08 land and vegetation product for the ICESat-2 Mission. **2019**, 1–13.
43. Neuenschwander, A.; Pitts, K. The ATL08 land and vegetation product for the ICESat-2 Mission. *Remote Sens. Environ.* **2019**, *221*, 247–259, doi:10.1016/j.rse.2018.11.005.